Extended Abstracts of the 2015 International Conference on Solid State Devices and Materials, Sapporo, 2015, pp622-623

Gold Bowtie Aperture with Projected Pad Underneath and its Capability in Optical Sensing

Peng-Yu Chen*, Tsan-Wen Lu, and Po-Tsung Lee

Department of Photonics, National Chiao Tung University
Rm. 401 CPT Building, 1001 Ta-Hsueh Rd., Hsinchu 30010, Taiwan
Phone: +886-3-5712121 ext. 59341 E-mail: pon653656@yahoo.com.tw

Abstract

We propose a gold nanostructure that can be realized via simplified fabrication without lift-off process, named bowtie aperture with projected pad underneath. Two localized surface plasmon resonance modes are identified in simulations and experiments. For optical index sensing, ultrahigh sensitivity of 1620 nm/RIU is experimentally demonstrated via our presented design.

1. Introduction

Surface plasmon polariton (*SPP*), the electron oscillation at the metal/dielectric interface, can produce a highly concentrated and a fast-decaying optical field near and away from the interface, respectively. This *SPP* wave confined via various metallic nanostructures in a dielectric system results in localized surface plasmon resonance (*LSPR*) [1]. Owing to its highly enhanced field concentrating near the structure surface, *LSPR* is very beneficial for applications requiring strong interaction between light and surrounding medium, for example, optical sensing [2]. By optimizing the topology of metallic nanostructure, *LSPR* can be further enhanced via different efforts, for example, lightning-rod and gap effects in nano-bowtie with tip and gap structures [3]. Based on the nano-bowtie structure, in this report, we propose a novel *LSPR* design, named bowtie aperture with projected pad underneath (*BAPPU*). Comparing with the conventional nano-bowtie structure, this design can be easily fabricated without lift-off process. In addition to analyzing the *LSPRs* in our presented *BAPPU* design, their capabilities of optical sensing will be also investigated.

2. Experiments

Design and Fabrication of Gold BAPPU

As shown in Fig. 1(a), our proposed gold *BAPPU* consists of a gold bowtie pad on SiO_2 (with refractive index of 1.45) substrate and a gold bowtie aperture above the pad. A photo-resist layer (*ZEP*-520, with refractive index of 1.54 and thickness h of 100 nm) serves as a spacing layer between the aperture and the pad. This structure can be simply realized via depositing gold film (with thickness h_g of 30 nm) on the photo-resist layer with hollow bowtie shape patterned by electron-beam (e-beam) lithography, as illustrated in the inset of Fig. 1(a). Its easiness in fabrication would be beneficial for integration on chips or fiber tips [4]. Top-view and zoom-in scanning electron microscope (*SEM*) pictures of gold *BAPPU* array are shown in Fig. 1(b).

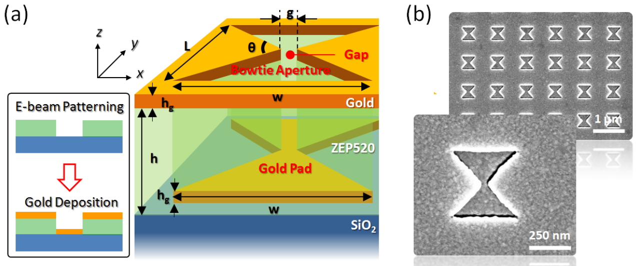

Fig. 1 (a) Schematic, structural parameters, and fabrication process of gold *BAPPU*. (b) Top-view and zoom-in *SEM* pictures of fabricated gold *BAPPU* array.

Theoretical and Experimental Mode Analysis in Gold BAPPU

To analyze the *LSPRs* in gold *BAPPU*, 3D finite element method (*COMSOL* Multiphysics software package) with Lorentz-Drude model for fitting the dielectric function of gold is employed. As defined in Fig. 1(a), the width (w) and length (L) of bowtie aperture/pad are set as 400 and 395 nm, respectively. In addition, considering the feasibility in fabrication, the gap size g of bowtie aperture/pad is set as 30 nm. The *LSPRs* are then excited by an x-polarized (parallel to the gap) plane wave incident from SiO_2 substrate along z-direction. Theoretic reflection spectrum of gold *BAPPU* is shown in Fig. 2(a). Two *LSPR* dips, fundamental and high order modes, are observed at 2710 and 1490 nm, respectively. Theoretic mode profiles in $log|E|$ fields of these two modes in aperture and on pad are shown in Fig. 2(b). These two modes can be classified into fundamental and high order modes according to their electric

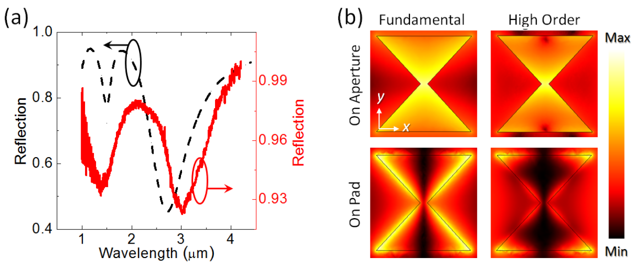

Fig. 2 (a) Theoretic (dash line) and experimental (red line) reflection spectra from gold *BAPPU* via x-polarized excitation waves. (b) Theoretic $log|E|$ fields of the fundamental and high order modes at the xy-plane centered in the bowtie aperture and 5 nm above the bowtie pad.

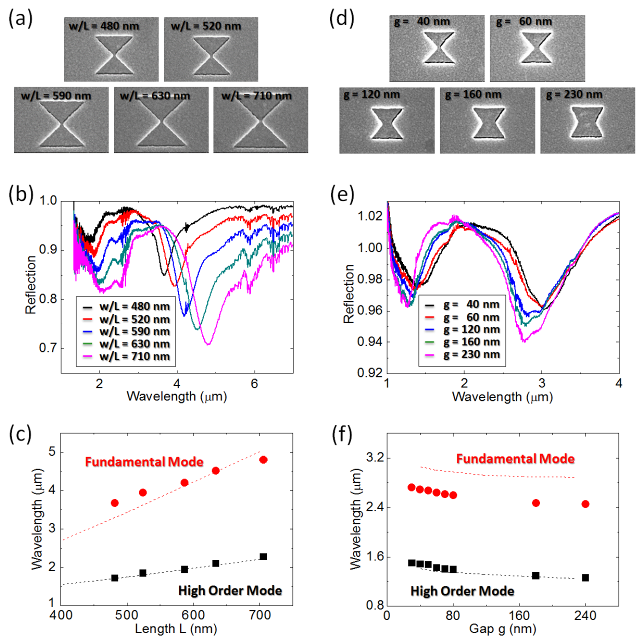

Fig. 3 (a) (d) Zoom-in *SEM* pictures and (b) (e) measured reflection spectra of *BAPPU* with varied *w*/*L* and *g*. (c) (f) Theoretical (dash-lines) and measured wavelengths of the fundamental and high order modes in *BAPPU* with different *w*/*L* and *g*.

field distributions along the pad edges. In bowtie aperture, owing to lightning-rod and gap effects, the mode fields are mainly enhanced and concentrated near the gap regions. Both in aperture and on pad, the fundamental mode shows stronger electric fields than the high order mode. Measured reflection spectra from gold *BAPPU* with the parameters in simulation is shown in Fig. 2(a). Two *LSPR* dips agreed with the simulation results are observed at 3015 and 1380 nm, which can be initially identified as the fundamental and high order modes.

To further identify these two modes, at first, the *w* and *L* of *BAPPU* are changed simultaneously. The zoom-in *SEM* pictures of gold *BAPPU* with varied *w*/*L* from 480 to 710nm (*g* is fixed at 30 nm) and the measured reflection spectra are shown in Figs. 3(a) and (b), respectively. Both the fundamental and high order modes show red shift with increasing *w*/*L*. Their variation trends in wavelength quite agree with the simulation results, as shown in Fig. 3(c). In addition, we also change the gap size *g* of *BAPPU*. The zoom-in *SEM* pictures of gold *BAPPU* with *g* = 40 - 230 nm (*w*/*L* are fixed at 400 nm) are shown in Fig. 3(d). The measured reflection spectra are in Fig. 3(e). Both the fundamental and high order modes show blue shift with increasing *g*. Again, their variation trends in wavelength agree with the simulation results, as shown in Fig. 3(f). Therefore, we can identify these two dips in spectra as the fundamental and high order modes.

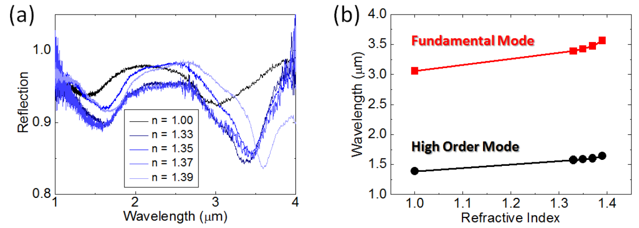

Fig. 4 (a) Measured reflection spectra of gold *BAPPU* under different surrounding refractive indices ranging from 1.00 to 1.39. (b) Wavelengths of the fundamental and high order modes under different refractive indices.

Optical Sensing via Gold BAPPU

Owing to the highly concentrated field within the aperture, *LSPRs* in gold *BAPPU* will be beneficial for optical sensing. For *BAPPU* with *w*/*L* and *g* of 400 and 40 nm, refractive index of the surrounding medium is changed from 1.00 to 1.39 in simulations and experiments. The measured reflection spectra are shown in Fig. 4(a). Both fundamental and high order modes exhibit significant red shift with the increased refractive index. As shown in Fig. 4(b), by fitting their wavelength variation, the fundamental mode shows a very high sensitivity of 1620 nm per refractive index unit (nm/*RIU*). This value agrees with theoretical sensitivity (~ 1660 nm/*RIU*) of the fundamental mode quite well. In contrast, the high order mode shows a lower sensitivity of 780 nm/*RIU*. Thus, for optical sensing application via the gold *BAPPU* design, the fundamental mode will be a better candidate than the high order mode. Nevertheless, the sensitivities of these two modes are still significantly higher than that (~ 125 nm/*RIU*) in similar configuration using nano-hole aperture with projected nano-disk underneath [4].

3. Conclusions

In this report, we propose and demonstrate gold *BAPPU* with *LSPRs*, which can be easily fabricated without the lift-off process. Its easiness in fabrication would be beneficial for integration on chips or fiber tips. Two different *LSPR* modes, the fundamental and high order modes, are well identified both in simulations and experiments. Both of them show extremely concentrated fields near the gap regions in aperture. For optical index sensing, the fundamental and high order modes exhibit very high sensitivities of 1620 and 780 nm/*RIU*, respectively. Based on above features, we believe our presented gold *BAPPU* design can be a potential candidate for lab-on-fiber optical sensors.

References

[1] E. Ozbay, Science **311** (2006) 189.
[2] K. M. Mayer and J. H. Hafner, Chem Rev. **111** (2011) 3828.
[3] D. P. Fromm, A. Sundaramurthy, P. J. Schuck, G. Kino, and W. E. Moerner, Nano Lett. **4** (2004) 957.
[4] M. Consales, A. Ricciardi, A. Crescitelli, E. Esposito, A. Cutolo, and A. Cusano, ACS Nano **6** (2012) 3163.